A mapping label required for normal scale of body representation in the cortex

Pierre Vanderhaeghen[1,2], Qiang Lu[1], Neal Prakash[3], Jonas Frisén[4], Christopher A. Walsh[5], Ron D. Frostig[3] and John G. Flanagan[1]

[1] *Department of Cell Biology and Program in Neuroscience, Harvard Medical School, Boston, Massachusetts 02115, USA*

[2] *Present address: Institute of Interdisciplinary Research, University of Brussels, B-1070 Brussels, Belgium*

[3] *Department of Neurobiology and Behavior and Center for the Neurobiology of Learning and Memory, University of California at Irvine, Irvine, California 92697, USA*

[4] *Department of Cell and Molecular Biology, Medical Nobel Institute, Karolinska Institute, S-171 77 Stockholm, Sweden*

[5] *Division of Neurogenetics, Department of Neurology, Beth Israel Deaconess Medical Center, Boston, Massachusetts 02115, USA*

The first two authors contributed equally to this work.

Correspondence should be addressed to J.G.F. (flanagan@hms.harvard.edu)

The neocortical primary somatosensory area (S1) consists of a map of the body surface. The cortical area devoted to different regions, such as parts of the face or hands, reflects their functional importance. Here we investigated the role of genetically determined positional labels in neocortical mapping. Ephrin-A5 was expressed in a medial > lateral gradient across S1, whereas its receptor EphA4 was in a matching gradient across the thalamic ventrobasal (VB) complex, which provides S1 input. Ephrin-A5 had topographically specific effects on VB axon guidance *in vitro*. Ephrin-A5 gene disruption caused graded, topographically specific distortion in the S1 body map, with medial regions contracted and lateral regions expanded, changing relative areas up to 50% in developing and adult mice. These results provide evidence for within-area thalamocortical mapping labels and show that a genetic difference can cause a lasting change in relative scale of different regions within a topographic map.

The layout of the neocortical surface reflects its functions. For example, the primary somatosensory area (S1) consists of a topographic map of the body surface, in which different parts of the body are represented at different scales[1,2]. The scale of such features varies between species, and even individuals, in a manner that reflects functional importance and probably contributes to differences in functional ability[1–8].

Such topographic organization requires corresponding patterning of incoming and outgoing connections. One mechanism for topographic patterning of connections is correlated neural activity. In visual cortex, neural activity and visual experience are important for normal development of ocular dominance and orientation columns[9–11]. In somatosensory cortex, the innervation density of body regions is approximately correlated with the size of their cortical representations, suggesting that the scale of representation could be determined simply by the amount of neural input[1,2,12]. Supporting this idea, reducing activity during development, for example by cutting a nerve or trimming a rodent's whiskers, can change the input map in S1 (ref. 13). Furthermore, although initial attempts at drug inhibition of activity did not obviously affect rodent S1 development[13], pharmacological or genetic disruption of the NMDA receptor impairs barrel map formation and plasticity[13–15].

Activity-independent mechanisms are postulated to establish an initial rough map, which would then be remodeled to the final form by activity[11,16]. However, the role of activity-independent mechanisms in the neocortex is not well understood. One potential mechanism could rely on timing: the thalamus and cortex show maturation gradients, which could be translated into spatial differences as axons reach their target[17,18]. An alternative could be complementary mapping labels on thalamic axons and their targets[19]. However, *in vitro* studies reveal no area-specific cues in the neocortex[20]. Moreover, thalamic afferents can form distinctive somatosensory or auditory maps when induced to innervate inappropriate cortical areas[21,22], emphasizing the prominent influence of incoming axons, and suggesting that the neocortex itself may have little instructive role.

Ephrins and their Eph receptors seem to be topographically specific mapping labels in the retina and its subcortical targets[23–27]. Here we investigate their role in neocortical map development. Based on expression patterns or *in vitro* assays, suggested roles include determining layer specificity of intracortical connections[28] or specificity of connections to distinct areas in limbic cortex or neocortex[29–31].

Our results show ephrin-A5 can regulate topographic organization of the neocortex. Ephrin-A5 is expressed in a gradient across S1. The thalamic VB complex has a complementary receptor gradient, and its axons respond topographically to ephrin-A5 *in vitro*. In mice lacking the ephrin-A5 gene, S1 thalamocortical connections seemed largely normal, but there was a graded topographically specific distortion, which was not seen at subcortical levels and persisted from development into

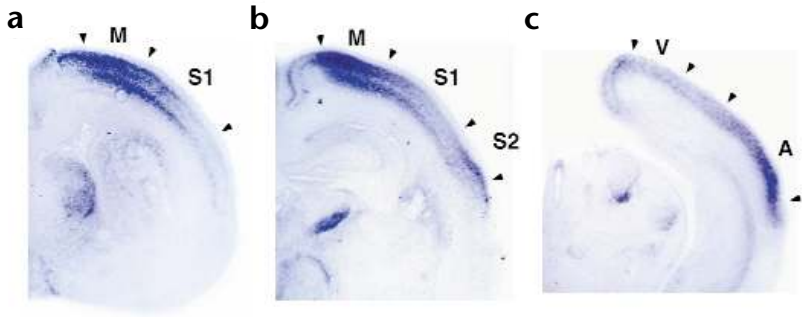

Fig. 1. Ephrin-A5 RNA expression within motor and sensory areas of the developing rodent neocortex. Coronal sections through anterior (**a**), middle (**b**) and posterior (**c**) P1 rat neocortex show gradients of expression across the cortical plate in motor (M), primary somatosensory (S1), secondary somatosensory (S2) and primary auditory (A) areas. Expression in the primary visual area (V) was weak and not obviously graded. Areas were identified by Nissl and AChE staining of alternate sections.

adulthood. The results provide evidence for within-area thalamocortical mapping labels. They also indicate that genetically determined labels can have a lasting influence on the relative scale of different regions within a map.

Results

Ephrin-A5 layer specificity and gradients in cortical areas

We began by examining RNA expression of all five known ephrins of the A subfamily, the subset most clearly implicated in subcortical mapping, during the time thalamocortical axons grow into the cortex. These results are mostly consistent with other studies of ephrin expression in rodent cortex[28,29,31], although a potential relationship of the patterns to within-area tangential mapping has not been described. Cortical expression of ephrin-A2 RNA appeared moderate but uniform, and ephrin-A3 was moderately expressed in cortical plate and subplate, though we did not see obvious gradients. However, we were struck by the prominent, patterned expression of ephrin-A5 RNA.

The timing and layer specificity seemed consistent with a role in map development. Ephrin-A5 RNA was detected in cortical plate from embryonic day (E)19 to postnatal day (P)3 in rat and E18 to P3 in mouse (**Figs. 1** and **2**). The onset of expression preceded the massive invasion of the cortical plate by thalamocortical axons, assessed by co-staining for acetylcholinesterase (AChE), an early marker for thalamocortical axons in rat, as well as patterning of thalamocortical axons into whisker barrels, first detectable around P0 (refs. 13, 32; **Fig. 2a–i**). Expression was seen prominently in layers VI and IV, with some layer V expression especially in the motor areas. This again seems consistent with a role in the mapping of thalamocortical axons, as their patterning is thought to occur initially in the deep layers and then to be transferred and refined in layer IV (refs. 13, 32).

The ephrin-A5 pattern across the plane of the cortical plate suggested a potential role as a tangentially specific label. Expression was prominent in the primary somatosensory and motor areas in a single medial > lateral gradient (**Fig. 1a** and **b**), in the primary auditory area in an opposite lateral > medial gradient (**Fig. 1c**), and in the secondary somatosensory area in a lateral > medial gradient (**Fig. 1b**), but was weak and not obviously graded in the primary visual area (**Fig. 1c**). We focus here on the primary somatosensory area, particularly the posteromedial barrel subfield (PMBSF), the map of the main whisker pad, where the whisker barrels provide well characterized markers of map topography. The prominent medial > lateral gradient of ephrin-A5 RNA was seen from E19 to P1 (**Fig. 2a–m**). No obvious anterior–posterior gradient was seen on parasagittal or horizontal sections (data not shown). This gradient encompassed the PMBSF, visible by its barrel staining pattern, and also included more medial regions corresponding to the rest of the body (**Fig. 2l** and **m**). At P3, a trend of differential expression could still be seen, along both the barrel rows and arcs, with an overall medial > lateral distribution (**Fig. 2n–s**). However, at P3 there was a discontinuous pattern of ephrin-A5 staining that seemed to correspond to the barrel pattern, especially in layer VI in sections cut across the rows (**Fig. 2p** and **q**). This was further assessed on tangential sections of P3 flat mounts (**Fig. 2t**), revealing patches of expression strikingly reminiscent of the histochemically stained somatosensory map, including components such as forelimb, hindlimb and whisker barrels. This observation has no obvious precedent in work on ephrins in subcortical projections, and indicates that at late mapping stages ephrin-A5 becomes concentrated in the regions innervated by thalamocortical axons.

To detect ligand protein distribution, we used affinity probe *in situ*[33], with probes consisting of soluble Eph receptor ectodomains fused to alkaline phosphatase (AP). A medial > lateral gradient was seen across the motor and somatosensory cortex, similar to the pattern of ephrin-A5 RNA (**Fig. 2u–x**). However, in ephrin-A5$^{-/-}$ mice, a similar though less intense gradient was still seen. This implies there are overlapping gradients of more than one ephrin, as in subcortical maps[23,24,34]. It also implies that any corresponding phenotype in the ephrin-A5$^{-/-}$ mice is likely to result from a change in slope or height, rather than a total deletion, of the overall composite gradient of ephrins.

EphA4 gradient across somatosensory VB complex

In maps formed by retinal axons, in addition to an ephrin gradient across the target[23,24,26,27], a matching Eph receptor gradient is found across the retina[23,27], giving ligand and receptor the distributions expected of complementary topographic mapping labels. We therefore tested for Eph receptor expression in the VB complex, the main thalamic relay to S1. Of the four receptors tested (EphA3, EphA4, EphA5 and EphA7), only EphA4 RNA was highly expressed in VB, from at least E18 to P3, in a ventromedial > dorsolateral gradient, within both VPM and VPL, the trigeminal and dorsal column components of the VB respectively (**Fig. 3a–i**). Compared with the somatosensory map in VPM[35], the orientation of the EphA4 gradient is such that levels are highest in the part corresponding to the anterior snout and high-numbered arcs of the PMBSF, located laterally in S1. This orientation could therefore be consistent with a repellent ligand-receptor interaction in thalamocortical mapping, as proposed in retinal maps[23–27,34]. By P3, the EphA4 RNA gradient started to fade, and in the VPM it now appeared in a discontinuous pattern similar to the cytochrome oxidase barreloid pattern (**Fig. 3g** and **h**), and reminiscent of the barrel-like pattern of cortical ephrin-A5 at this stage.

The expression pattern of Eph receptors at the protein level was tested by affinity probe *in situ* with an ephrin-A5–AP fusion

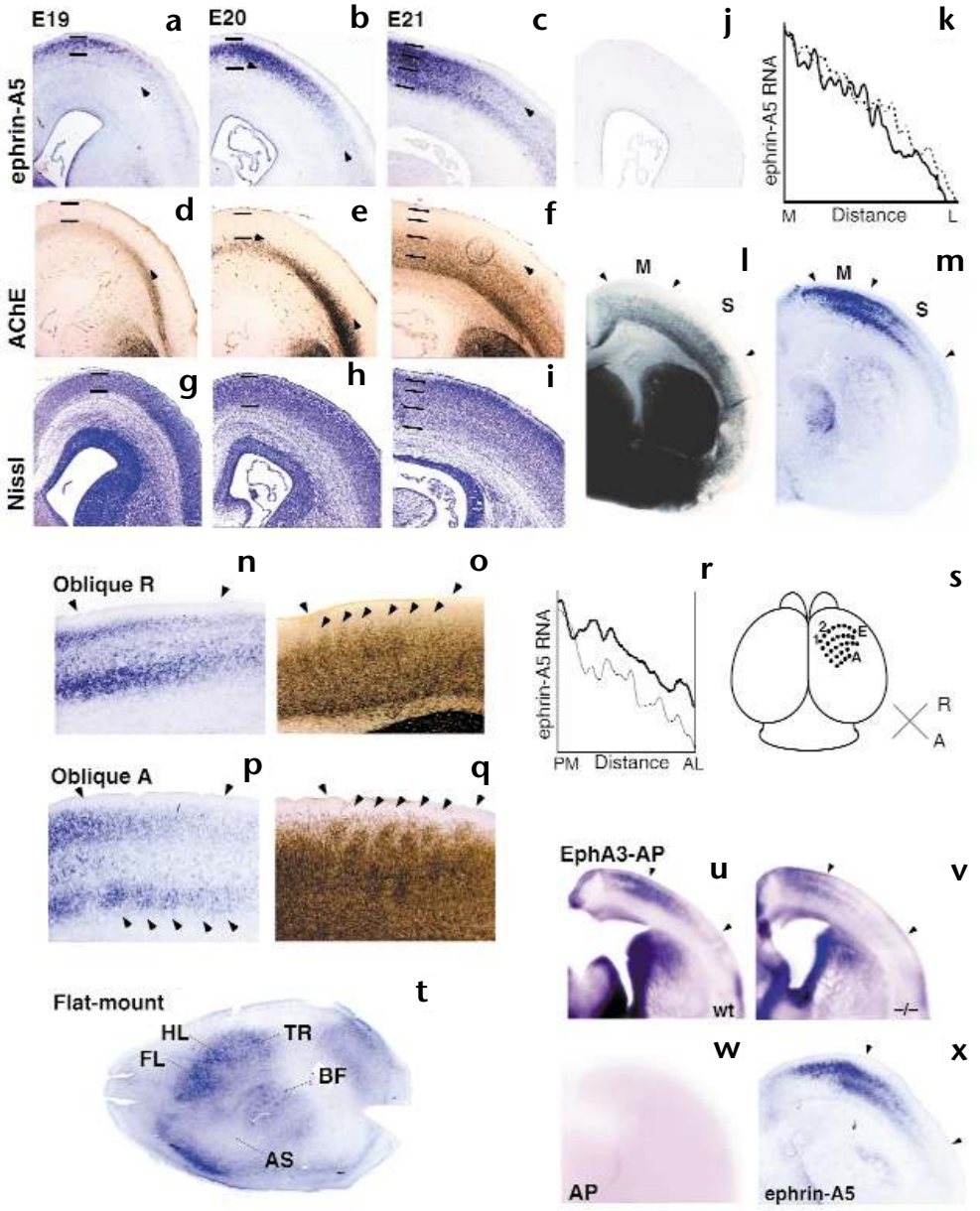

Fig. 2. Ephrin-A5 graded expression across the developing rodent somatosensory cortex. (**a–j**) Coronal sections of embryonic rat brain, showing ephrin-A5 RNA in the somatosensory cortex at E19 (**a**), E20 (**b**) and E21 (**c**), compared on adjacent sections with the ingrowth of thalamocortical axons, stained by AChE (**d–f**) and development of the cortical plate, Nissl stained (**g–i**). Arrowheads indicate the most superficial extent of thalamocortical axons visible by AChE. Bars show extent of the cortical plate at E19 and E20, or boundaries between presumptive layers IV, V and VI at E21. (**j**) Control section of E20 rat brain treated with ephrin-A5 sense probe. (**k**) Densitometric scan showing medial (M) to lateral (L) graded expression of ephrin-A5 RNA across the somatosensory area. Results from two independent E20 sections are shown; the *y*-axis is in arbitrary units. (**l, m**) Coronal sections of P1 rat brain, showing layer IV barrels stained with AChE (**l**), compared with expression of ephrin-A5 in the motor (M) and somatosensory (S) areas (**m**), delineated by arrowheads. (**n–q**) Oblique sections cut along the rows (**n, o**) or the arcs (**p, q**; medial is left) of the P3 rat PMBSF, showing ephrin-A5 RNA (**n, p**) or AChE staining (**o, q**). Arrowheads indicate the barrel-like discontinuous pattern of AChE and ephrin-A5. (**r**) Densitometric scan showing a posteromedial (PM) to anterolateral (AL) graded expression of ephrin-A5 along the rows of the barrel field in layers VI (bold line) and IV (thin line). (**s**) Schematic representation of the row (R) and arc (A) oblique section planes in relation to the PMBSF. (**t**) Section of flat-mounted P3 rat cortex, showing a discontinuous pattern of ephrin-A5 RNA reminiscent of the body map. FL, forelimb; HL, hindlimb; BF, posteromedial barrel subfield; TR, trunk. Little staining is seen in the anterior snout (AS) region, located laterally. (**u–x**) Coronal sections of P0 mouse brain, showing binding *in situ* with EphA3–AP probe in the somatosensory cortex of wild-type (**u**) and ephrin-A5$^{-/-}$ (**v**) mouse. (**w**) Control with AP only. (**x**) Ephrin-A5 RNA in the cortex of a wild-type mouse for comparison. Arrowheads indicate the boundaries of the presumptive somatosensory cortex.

protein. Binding activity was detected on axons growing from VB explants *in vitro* (data not shown), and in embryos as early as E16 and up to P3, on thalamocortical axons en route to the cortex, through the internal capsule and in the subplate (**Fig. 3j**), confirming expression of Eph receptors on projecting thalamocortical axons.

Topographically specific effect of ephrin-A5 on VB axons

The *in vitro* stripe assay[36] was used to test for a guidance effect on VB axons. In contrast to the midbrain tectum, the ephrin-A5 gradient in S1 is restricted to a subset of layers and is not demarcated by major anatomical markers, making it difficult to set up an *in vitro* assay using native cortical membranes. However, we were able to test responses of VB axons to ephrin-A5 on transfected cell membranes. Axons from the ventromedial third of VB grew preferentially on stripes lacking ephrin-A5, indicating a repellent effect (**Fig. 3k**). Axons from the dorsolateral third had no preference, demonstrating topographic specificity (**Fig. 3k**). Stripe preference of each explant was scored on a 0 (no bias) to 4 scale. Ventromedial explants had a score of 1.86 ± 0.15

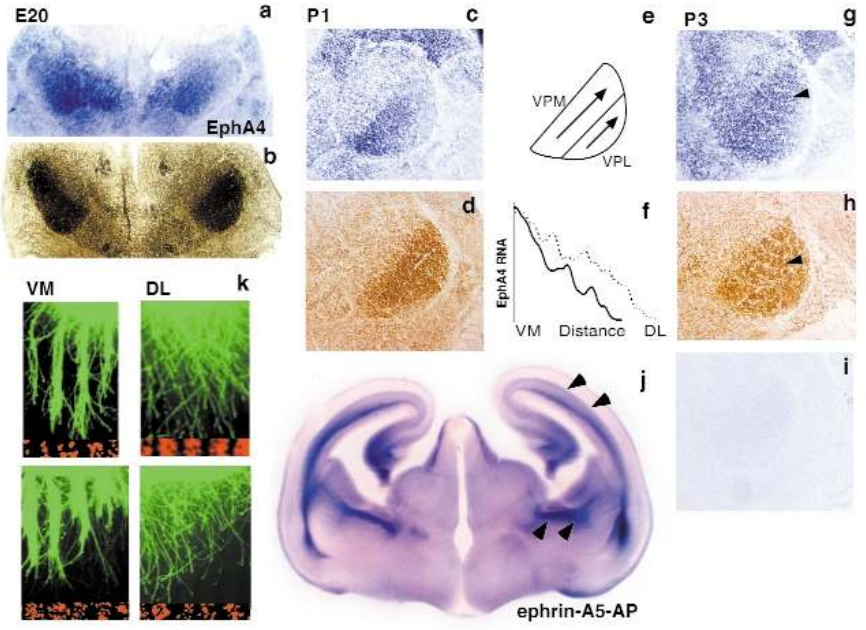

Fig. 3. The VB complex, the main somatosensory relay to the cortex, displays graded Eph receptor expression, and its axons are differentially repelled by ephrin-A5 *in vitro*. (**a–d, g–i**) Coronal sections of rat brain (medial is left in **c–i**), showing EphA4 RNA in VB at E20 (**a**), P1 (**c**) and P3 (**g**), compared with the VB markers AChE (**b**) and cytochrome oxidase (**d**, **h**). (**e**) Schematic representation of the ventromedial to dorsolateral gradient of EphA4 in the VPM and VPL portions of the VB. In (**g**) and (**h**), arrowheads indicate barreloid-like patterns. (**f**) Densitometric scan of the ventromedial (VM) to dorsolateral (DL) EphA4 RNA gradient in VPL (solid line) and VPM (dashed line). (**i**) Control EphA4 sense probe. (**j**) Ephrin-A5–AP binding *in situ* on E17 mouse brain. Arrowheads indicate staining of thalamocortical axons in the internal capsule and subplate. (**k**) *In vitro* stripe assay. Axons (green) from explants of ventromedial or dorsolateral VB are grown on alternating stripes of membranes from mock or ephrin-A5 transfected cells. Red fluorospheres mark lanes with ligand in upper panels, and without ligand in lower panels.

(mean ± s.e.) and dorsolateral explants a score of 0.1 ± 0.04 ($p < 0.001$). These results demonstrate ephrin-A5 can act *in vitro* as a repellent for VB axons, with a topographically appropriate preference for ventromedial axons.

Expansions and contractions in adult S1 map

Because the expression patterns and *in vitro* assays supported a role for ephrin-A5 in S1 map development, we characterized the map in ephrin-A5$^{-/-}$ mice[27]. We first used both retrograde and anterograde DiI labeling, an approach that reveals obvious abnormalities in the retinal maps in this mutant[26,27]. However, we were unable to find any abnormality in the somatosensory thalamocortical connections of early postnatal mice, in terms of layer specificity (assessed by anterograde labeling), area specificity or gross topographic arrangement (assessed by anterograde and retrograde labeling), with each labeling site mapping to a single projection site (**Fig. 4a–c** and data not shown). The precision of barrel-to-barreloid relationships in adult mice was further demonstrated in a separate study using intrinsic signal optical imaging (N.P., P.V., J.F., J.G.F. & R.F., unpublished data).

We next tested for changes in map layout, taking advantage of the excellent markers of topography provided by the whisker barrels. Cortical flat mounts of adult mice were analyzed by cytochrome oxidase staining, which shows the layout of the layer IV map of somatosensory input from the thalamus[13,18]. In mutants, the somatosensory map layout appeared grossly normal, containing representations of the major body parts and a normal number of PMBSF barrels (**Fig. 4d** and **e**).

However, there were significant changes in barrel dimensions. Moreover, these changes were not uniform, but showed a striking systematic variation, including contractions of some barrels and expansions of others (**Fig. 5**). Prominent contractions were found in medial PMBSF, especially the low-numbered D and E

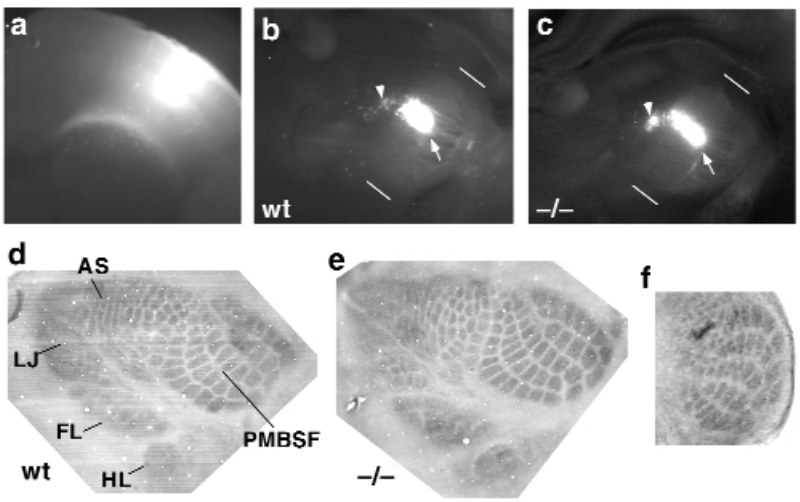

Fig. 4. Connectivity and pattern of the thalamocortical somatosensory map are grossly normal in ephrin-A5$^{-/-}$ mice. (**a–c**) DiI labeling of thalamocortical projections. (**a**) Coronal section through somatosensory cortex showing typical dye injection site. In wild-type (**b**) or ephrin-A5$^{-/-}$ mouse (**c**), a single cluster of retrogradely labeled cells (arrow) is found in the thalamic VB complex, in this case within the VPM nucleus (ventromedial and dorsolateral limits of VPM marked by oblique lines). A small additional cluster of labeled cells is found more medially in the POm complex (arrowhead). (**d**, **e**) Flattened sections of adult cortex stained for cytochrome oxidase, showing a grossly normal somatosensory pattern in wild-type (**d**) and ephrin-A5$^{-/-}$ (**e**) mouse. PMBSF, posteromedial barrel subfield; AS, anterior snout; LJ, lower jaw; FL, forelimb; HL, hindlimb. (**f**) Coronal section of P8 brainstem stained for cytochrome oxidase, showing an ephrin-A5$^{-/-}$ mouse with a normal pattern of barrelettes in the nucleus interpolaris.

rows. (Individual whiskers and their barrels are designated by a letter for the row and a number for the arc.) For example, the D1–E1 center-to-center barrel distance was reduced from 397.8 ± 5.1 μm to 329.8 ± 11.0 μm (–17%, $p < 0.001$). (Unless otherwise stated, all quantitations are for adult animals; wild type, $n = 8$; mutant, $n = 8$.) The contractions tended to diminish along both the rows and arcs, in an overall medial to lateral trend, and then shifted into expansions, particularly in the A and B rows (A1–B1 distance increased from 309.0 ± 8.2 μm to 348.0 ± 8.3 μm, +13%, $p = 0.004$) and the high-numbered C, D and E rows (D8–E8 distance increased from 268.0 ± 5.0 μm to 319.9 ± 6.3 μm, +19%, $p < 0.001$). In terms of cortical surface area, the relative space devoted to different parts of the map changed by up to approximately 50%. (For example, the area of the D7–D8–E7–E8 cluster, divided by the E1–E2–D1–D2 area, increased from a ratio of 0.501 ± 0.005 to 0.753 ± 0.003, +51%, $p < 0.001$.) However, total PMBSF area was not significantly changed (wild type, 1.94 ± 0.17 mm^2; mutant, 1.98 ± 0.13 mm^2, $p = 0.86$). The medial-to-lateral trend in the shift from contractions to expansions (**Fig. 5**) was strikingly similar to the ephrin-A5 gradient at earlier ages.

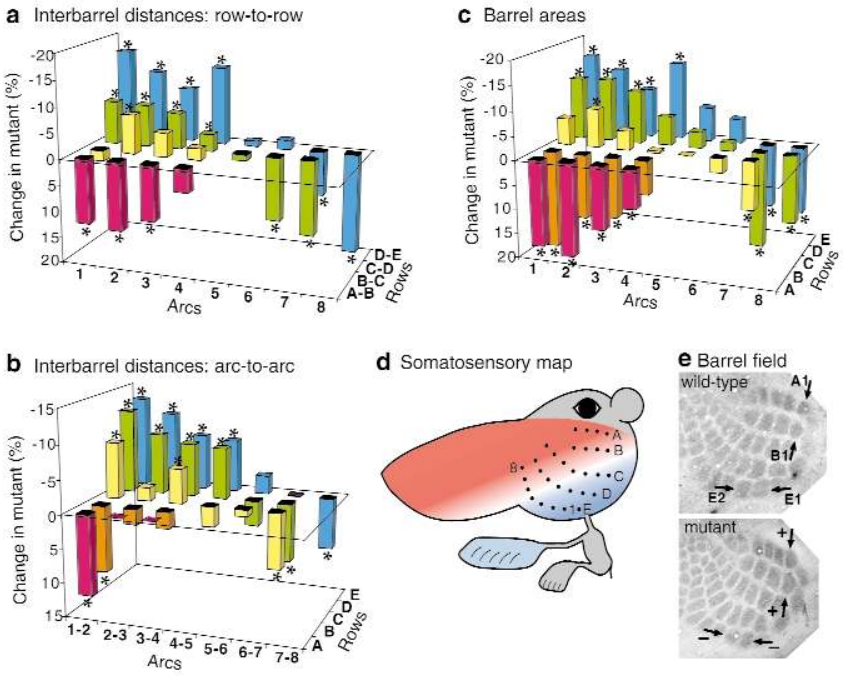

Fig. 5. Expansions and contractions in the cortical somatosensory map of ephrin-A-5$^{-/-}$ mice. Center-to-center distances between pairs of barrels (**a**, **b**) and areas of individual barrels (**c**), in the main whisker pad map (posteromedial barrel subfield, PMBSF). Each bar shows the percentage change in mean value, for a group of adult ephrin-A5$^{-/-}$ mice ($n = 8$) compared with wild-type mice ($n = 8$). Statistically significant changes ($p < 0.05$) are indicated by an asterisk. Colors demarcate different barrel rows. (**d**) Schematic representation of the distortions in the somatosensory map. Head, trunk, forelimb and hindlimb representations are shown, with whisker barrels in the PMBSF indicated by dots and identified conventionally by a letter for the row and a number for the arc. Red, expansions; blue, contractions; gray, regions not quantitated. (**e**) PMBSF map from a wild-type and an ephrin-A5$^{-/-}$ cortex, stained for cytochrome oxidase. Arrows indicate examples of barrel pairs that are expanded (+) or contracted (–) in the mutant.

Regions outside the PMBSF are harder to quantify because there are few well-defined landmarks. However, we were able to measure the length of the anterior snout representation, which in mutants was expanded (from 2200 ± 30.5 μm to 2368 ± 16.8 μm, +7.6%, $p = 0.003$), and the length of the forelimb representation, which was reduced (from 1784 ± 13.5 μm to 1683 ± 11.4 μm, –5.7%, $p = 0.001$), consistent with the trend of contractions medially and expansions laterally (**Fig. 5d**). No difference was found between mutants and controls in other morphometric parameters, such as brain weight, cortical layering, body or snout shape, or size and shape of the cerebral hemispheres, except that the body weight of mutants was slightly increased (from 28.02 ± 0.55 g to 29.95 ± 0.67 g, $p = 0.04$). Some mutants have a defect in neural tube closure (J.F. and M. Barbacid, unpublished results); the occasional mice that survived with midline head defects were excluded from the quantitative analysis here, although they did not appear to have any different phenotype in the cortical map.

Distortions of S1 arise during development

To test whether the S1 distortions in adult mice had already appeared at earlier developmental stages, we repeated the entire PMBSF analysis at P6, when cortical layering is reaching completion and the layer IV barrel map first becomes detectable in mice. The results revealed contractions and expansions that were quantitatively similar in percentage terms to those seen in adults. For example, the D1–E1 distance was reduced from 250.0 ± 3.6 μm in wild-type mice to 205.6 ± 6.0 μm in mutants (–18%, $p < 0.001$), and the A1–B1 distance was expanded from 189.6 ± 4.7 μm to 213.6 ± 4.8 μm (+13%, $p = 0.004$, wild type, $n = 7$; mutant, $n = 7$). The analysis of P6 mice thus indicates that the distortions in the layer IV input map appear during development, and also that they are not secondary to changes in the plexus of intracortical connections, which begins to develop only after P6 (refs. 28, 37).

Similar distortions were not seen at subcortical levels

In principle, a change in the cortical map could be explained by a corresponding change at subcortical or peripheral levels. In the brainstem trigeminal nuclei, especially the nucleus interpolaris, cytochrome oxidase staining reveals a stereotypic pattern of barrelettes (**Fig. 4f**). Here we were not able to detect any difference between mutants and controls. For example, the D1–E1 distance was 206.4 ± 3.4 μm in wild-type mice and 205.4 ± 2.6 μm in mutants ($p = 0.88$). Comparing the brainstem and cortex, the ratio of D1–E1 to A1–B1 distances was similar in the brainstem of controls (1.27 ± 0.02) and mutants (1.28 ± 0.03) and also in the cortex of controls (1.27 ± 0.04), whereas it was strongly reduced in the cortex of mutants (0.97 ± 0.05, –31%). These data provide no indication that the distortion in the cortex could be explained by a distortion at the brainstem level ($p < 0.001$ by two-way ANOVA, genotype × brain level). The same conclusions were reached from measurements throughout the barrelette map in the nucleus interpolaris.

The map in the thalamic VB nucleus was harder to quantify because the barreloid organization curved in three dimensions. However, we were able to reproducibly measure the distance from the anterior end of the lower jaw representation to the barreloids of arc 1. This distance was expanded in the cortex (average distance from lower jaw to arc 1 barrels was 3491 ± 26 μm in wild types, versus 3664 ± 35 μm in mutants, +5.1%, $p = 0.001$), but was not significantly affected in the thalamus (1164 ± 19 μm in wild types, $n = 9$, and 1124 ± 28 μm in mutants, $n = 9$, $p = 0.28$). These results provide no indication that the distortion in the cortex could be explained by a distortion at the thalamic level ($p < 0.001$ by two-way ANOVA).

Discussion

Ephrins as positional labels in neocortical mapping

It has been unclear whether positional labels contribute to patterning of sensory inputs across the neocortex. Furthermore, because the neocortex initially seems uniform, it has been unknown whether such labels might be expected in area-specific patches, gradients across the whole cortex, within-area gradients or some other distribution.

We showed that ephrin-A5 is expressed in a prominent gradient across S1. This gradient, the timing and layer specificity of expression, and the matching EphA4 gradient across the thalamic VB complex all seem to fit the idea that ephrin-A5 and EphA4 could act as complementary within-area mapping labels for somatosensory thalamocortical projections. *In vitro* support comes from stripe assays showing ephrin-A5 causes topographically specific repulsion of VB axons. *In vivo* support comes from the graded, topographically specific expansions and contractions in the thalamocortical input map of both developing and adult ephrin-A5$^{-/-}$ mice. These distortions in the mutant could be accounted for by a medial shift in thalamocortical axon termination zones, toward the direction normally occupied by high levels of repellent ephrin-A5. If other influences tend to hold the S1 boundaries fixed, the expected result would be map compression medially and expansion laterally, as observed.

Ephrin-A5$^{-/-}$ adult mice were also characterized by intrinsic signal optical imaging, to quantify whisker-evoked activity patterns (N.P., P.V., J.F., J.G.F. & R.F., unpublished data). In terms of the input map, there were changes in the locations of selected whisker functional representations consistent with the changes in whisker barrel locations seen here. In terms of intracortical processing, the area occupied by individual whisker functional representations showed no detectable change, whereas there were changes in the overlap between pairs of whisker representations. Thus, in addition to addressing intracortical processing, the functional imaging results agree with the analysis here in identifying changes in the S1 input map.

Although ephrin-A5 could have additional roles in the somatosensory system, it is unlikely that the distortions seen here in the thalamocortical map are caused entirely by changes at intracortical, subcortical, peripheral or behavioral levels for several reasons. First, map distortions could not be detected at the level of thalamic or brainstem relays. This contrasts with peripheral manipulations before the critical period in rodents up to P0, which affect both brainstem and cortical maps[13,38–40]. Second, we see distortions in cortical layer IV, contrasting with peripheral manipulations in early postnatal rodents, which do not distort the histochemical map of afferents in layer IV, even though there can be electrophysiological changes, particularly in layers II and III (refs. 40, 41). Third, the distortion correlates with the prominent cortical ephrin-A5 gradient, whereas the pattern of ephrin-A5 expression in brainstem and thalamic somatosensory nuclei provides no evident explanation for the observed distortions (refs. 27, 29, 42 and unpublished observations). Fourth, the S1 distortions did not alter noticeably with age, and had occurred by P6, while the layer IV input map is emerging, but before the plexus of intracortical connections has developed. Fifth, the distortion includes both barrel-field and forelimb representations, which are adjacent in cortex but separate in subcortical trigeminal and dorsal column pathways, again contrasting with peripheral manipulations[40].

In addition to S1, we found ephrin-A5 expression gradients across the cortical plate within the motor, auditory and secondary somatosensory areas, suggesting a broader role as a within-area topographic label. The earlier expression of ephrins in the cortical ventricular and subventricular zones has also suggested roles in initially setting up cortical pattern[30,31], although this would not seem to provide an explanation for the medial–lateral distortion we see here, as early ephrin-A5 expression is in an anterior–posterior gradient[31]. Ephrins could also be involved in setting up layer specificity, or selectivity of thalamocortical axons between different areas of the neocortex or limbic cortex[28,29]. Although our studies on the ephrin-A5$^{-/-}$ mice did not provide support for these ideas, we did not test them exhaustively, and such roles might be obscured by molecular redundancy.

A role for ephrin-A5 as a within-area topographic mapping label for thalamocortical connections seems very consistent with proposals of ephrin action in retinal maps[23–27,34]. However, in studies of retinal maps in the ephrin-A5$^{-/-}$ mutant, focal DiI injections in the retina reveal some axons projecting to the correct location, and others to incorrect or multiple locations[26,27]. In contrast, the cortical somatosensory map shows no obvious loss of point-to-point precision, but is systematically distorted. The maintenance of a precise map could in principle be explained by alternative types of mapping mechanism, or by the overlapping ephrin gradients that were seen here with a receptor-AP probe. These ideas could ultimately be tested by removal of multiple ephrins from the cortex; in the meantime, the full extent of the ephrins' role remains unknown.

Our results have implications for the upstream mechanisms that set up cortical patterning. It has been unclear to what degree the fates and connectivity of cortical cells may be predetermined in the neuroepithelium, or determined by incoming influences such as the afferent thalamocortical axons—alternatives emphasized respectively in the protomap and protocortex models[43,44]. An important role for thalamocortical input is shown by cortical rewiring studies[21,22]. On the other hand, some cortical markers show region-specific expression even when thalamic axons fail to reach the cortex, indicating patterning within the cortex[45]. Ephrin-A5, in addition to providing a marker of cortical cell fate, seems to serve as a positional label for map formation. We find the S1 gradient of ephrin-A5 appears before any obvious invasion of the cortical plate by incoming thalamocortical axons, supporting the idea that, in addition to cortical fates, at least some aspects of cortical connectivity can be determined by programs intrinsic to the cortex.

Genetic control of scale within a map

Previous work has been consistent with the idea that the relative scale of different features within the cortical somatosensory maps, as well as visual and auditory maps, could be determined entirely by the level of neural input from the periphery[1,2,12]. Our find-

ings now indicate that a genetic change of positional labels within the brain can change the relative area allocated to different regions within a map without obviously disrupting to the map's integrity. As far as we are aware, there is no precedent for such an observation, either in a cortical map or any other topographic map.

One implication is to indicate a new function for ephrins in mapping. Previous studies indicate that ephrins are topographic labels, in the sense that they can ensure orderly axonal projections, with neighbor relationships preserved. The results here indicate that the specific combination of ephrins can also determine relative scale of regions within a final map. In view of this, we would suggest the expression patterns of ephrins and Eph receptors may be adapted to appropriately mold the internal structure of maps. This model seems consistent with, and may explain, several notable features of ephrin expression in maps: individual maps contain multiple ephrins and Eph receptors in complex overlapping gradients[34]; different combinations of ephrins and Eph receptors are used in different maps[34]; and the combination used in a particular map can differ from one species to another[27]. These features could all serve to regulate internal map structure.

Finally, it has long been debated to what degree differences in neocortical properties may be determined by genetics versus environment[3,5,6,8,10,46,47]. The amount of cortical area devoted to a particular body region may determine functional ability, at least in part, as greater use and ability generally correlate with increased cortical representation[1–8]. Experience can undoubtedly be important in causing such differences between species and individuals. Although we have no direct evidence for a change in functional ability, our results show that a genetic difference in mapping labels can control the relative allocation of cortical surface area within a map, starting in development and persisting into adulthood.

Methods

***In situ* analysis.** Mouse RNA probes were as described[27,33]. Two nonoverlapping rat ephrin-A5 probes were amplified by PCR using primers from the published sequence[48] and gave indistinguishable results. E0 was defined as the plug date, and P0 as the day of birth. Brains were fixed with 4% paraformaldehyde overnight at 4°C for embryos or by perfusion postnatally. Hybridization was as described[27]; all results with antisense probes were compared with control sense probes and were confirmed by testing three to eight animals for each stage. Ephrin-A5–AP and EphA4–AP probes were used as described[23,27,33].

Somatosensory map organization. For retrograde labeling, tracer was injected using a Picospritzer II, animals were sacrificed one to two days later, fixed by perfusion, and brains were vibratome sectioned at 150 µm. Anterograde DiI labeling was on fixed oblique sections comprising VB and somatosensory cortex[32]. AChE and cytochrome oxidase staining were as described[49,50]. For quantitative analyses, after fixation by perfusion, tangential 100-µm sections of flattened cortices or coronal 50-µm sections of brainstem or thalamus were cytochrome oxidase stained, and digital camera images were quantified. For cortex, only cases with the entire PMBSF in one or two sections were analyzed to reduce variability due to angle of sectioning. For thalamus, distances from lower jaw to arc 1 were averaged through a complete series of coronal sections of one VB from each of 9 animals. Mice were a population of mixed C57BL/6 and 129/Sv strains[26]. To ensure differences were not due to strain background, barrels were measured in wild-type mice of the mixed population ($n = 8$), C57BL/6 ($n = 8$) and 129/Sv ($n = 8$) strains, and no significant differences were found. All values in the text were measured with similar results by a second investigator blind to genotype, and all comparisons are for age-matched animals. Except where otherwise stated, values are for adult mice, with $n = 8$ for ephrin-A5$^{-/-}$ and $n = 8$ for wild-type mice.

***In vitro* guidance assays.** Stable clonal 293T transfectants contained ephrin-A5 plasmid[27] or mock vector. The stripe assay[36] was used as described[25], except using as permissive substrate 33% to 66% membranes from P0–P3 rat lateral frontal cortex, which had no detectable binding for EphA4-AP. To make VB explants, including VPL and VPM, we collected E18–E20 embryos in oxygenated L15/0.6% glucose and removed the pia. Brains were embedded in 4% low melting agarose in L15, kept ice cold, and vibratome sectioned at 200 µm. Ventral and lateral VB boundaries could be seen on one to three sections under incident light; medial and dorsal boundaries were determined by comparing with similar sections stained with the VB marker AChE[50]. Accuracy was further ensured by comparing the dissected side with contralateral thalamus stained afterward with AChE; in all cases, explants contained VB and occasionally the most lateral part of VM. Explants were placed on stripes in Neurobasal/B27 medium and analyzed after 48 to 72 h.

Acknowledgements

We thank David Feldheim, Michael Hansen, Verne Caviness, David Van Vactor, Rick Born, Gerard Dallal, Sonal Jhaveri, Clay Reid and Michael Belliveau for help and advice. This work was supported by grants from the US NIH and NSF, the Swedish MRC, the Klingenstein foundation, the NATO/Belgian-American Educational Foundation and the Belgian FNRS.

Accepted 25 February 2000

1. Penfield, W. & Rasmussen, T. *The Cerebral Cortex of Man* (Macmillan, New York, 1950).
2. Woolsey, C. N. in *Biological and Biochemical Bases of Behavior* (eds. Harlow, H. F. & Woolsey, C. N.) 63–81 (Univ. of Wisconsin Press, Madison, Wisconsin, 1958).
3. White, L. E., Lucas, G., Richards, A. & Purves, D. Cerebral asymmetry and handedness. *Nature* **368**, 197–198 (1994).
4. Kaas, J. H. in *The Cognitive Neurosciences* (ed. Gazzaniga, M. S.) 51–71 (MIT Press, Cambridge, Massachusetts, 1995).
5. Riddle, D. R. & Purves, D. Individual variation and lateral asymmetry of the rat primary somatosensory cortex. *J. Neurosci.* **15**, 4184–4195 (1995).
6. Elbert, T., Pantev, C., Wienbruch, C., Rockstroh, B. & Taub, E. Increased cortical representation of the fingers of the left hand in string players. *Science* **270**, 305–307 (1995).
7. Buonomano, D. V. & Merzenich, M. M. Cortical plasticity: from synapses to maps. *Annu. Rev. Neurosci.* **21**, 149–186 (1998).
8. Howe, M. J. A., Davidson, J. W. & Sloboda, J. A. Innate talents: reality or myth? *Behav. Brain Sci.* **21**, 399–442 (1998).
9. Katz, L. C. & Shatz, C. J. Synaptic activity and the construction of cortical circuits. *Science* **274**, 1133–1138 (1996).
10. Hubel, D. H. & Wiesel, T. N. Early exploration of the visual cortex. *Neuron* **20**, 401–412 (1998).
11. Crair, M. C. Neuronal activity during development: permissive or instructive? *Curr. Opin. Neurobiol.* **9**, 88–93 (1999).
12. Welker, E. & Van der Loos, H. Is areal extent in sensory cerebral cortex determined by peripheral innervation density? *Exp. Brain Res.* **63**, 650–654 (1986).
13. O'Leary, D. D. M., Ruff, N. L. & Dyck, R. H. Development, critical period plasticity, and adult reorganizations of mammalian somatosensory systems. *Curr. Opin. Neurobiol.* **4**, 535–544 (1994).
14. Fox, K., Schlaggar, B. L., Glazewski, S. & O'Leary, D. D. M. Glutamate receptor blockade at cortical synapses disrupts development of thalamocortical and columnar organization in somatosensory cortex. *Proc. Natl. Acad. Sci. USA* **93**, 5584–5589 (1996).
15. Iwasato, T. *et al.* NMDA receptor-dependent refinement of somatotopic maps. *Neuron* **19**, 1201–1210 (1997).
16. Goodman, C. S. & Shatz, C. J. Developmental mechanisms that generate precise patterns of neuronal connectivity. *Cell* **72** (Suppl.), 77–98 (1993).
17. Molnar, Z. & Blakemore, C. How do thalamic axons find their way to the cortex? *Trends Neurosci.* **18**, 389–397 (1995).
18. Killackey, H. P., Rhoades, R. W. & Bennett-Clarke, C. A. The formation of a cortical somatotopic map. *Trends Neurosci.* **18**, 402–407 (1995).
19. Sperry, R. W. Chemoaffinity in the orderly growth of nerve fiber patterns and connections. *Proc. Natl. Acad. Sci. USA* **50**, 703–710 (1963).
20. Molnar, Z. & Blakemore, C. Lack of regional specificity for connections formed between thalamus and cortex in coculture. *Nature* **351**, 475–477 (1991).
21. Roe, A. W., Pallas, S. L., Hahm, J. O. & Sur, M. A map of visual space induced in primary auditory cortex. *Science* **250**, 818–820 (1990).
22. Schlaggar, B. L. & O'Leary, D. D. M. Potential of visual cortex to develop an array of functional units unique to somatosensory cortex. *Science* **252**, 1556–1560 (1991).

23. Cheng, H. J., Nakamoto, M., Bergemann, A. D. & Flanagan, J. G. Complementary gradients in expression and binding of ELF-1 and Mek4 in development of the topographic retinotectal projection map. *Cell* **82**, 371–381 (1995).
24. Drescher, U. *et al.* In vitro guidance of retinal ganglion cell axons by RAGS, a 25 kDa tectal protein related to ligands for Eph receptor tyrosine kinases. *Cell* **82**, 359–370 (1995).
25. Nakamoto, M. *et al.* Topographically specific effects of ELF-1 on retinal axon guidance in vitro and retinal axon mapping in vivo. *Cell* **86**, 755–766 (1996).
26. Frisen, J. *et al.* Ephrin-A5 (AL-1/RAGS) is essential for proper retinal axon guidance and topographic mapping in the mammalian visual system. *Neuron* **20**, 235–243 (1998).
27. Feldheim, D. A. *et al.* Topographic guidance labels in a sensory projection to the forebrain. *Neuron* **21**, 1303–1313 (1998).
28. Castellani, V., Yue, Y., Gao, P. P., Zhou, R. & Bolz, J. Dual action of a ligand for Eph receptor tyrosine kinases on specific populations of axons during the development of cortical circuits. *J. Neurosci.* **18**, 4663–4672 (1998).
29. Gao, P. P. *et al.* Regulation of thalamic neurite outgrowth by the Eph ligand ephrin-A5: implications in the development of thalamocortical projections. *Proc. Natl. Acad. Sci. USA* **95**, 5329–5334 (1998).
30. Donoghue, M. J. & Rakic, P. Molecular evidence for the early specification of presumptive functional domains in the embryonic primate cerebral cortex. *J. Neurosci.* **19**, 5967–5979 (1999).
31. Mackarehtschian, K., Lau, C. K., Caras, I. & McConnell, S. K. Regional differences in the developing cerebral cortex revealed by ephrin-A5 expression. *Cereb. Cortex* **9**, 601–610 (1999).
32. Agmon, A., Yang, L. T., O'Dowd, D. K. & Jones, E. G. Organized growth of thalamocortical axons from the deep tier of terminations into layer IV of developing mouse barrel cortex. *J. Neurosci.* **13**, 5365–5382 (1993).
33. Cheng, H. J. & Flanagan, J. G. Identification and cloning of ELF-1, a developmentally expressed ligand for the Mek4 and Sek receptor tyrosine kinases. *Cell* **79**, 157–168 (1994).
34. Flanagan, J. G. & Vanderhaeghen, P. The ephrins and Eph receptors in neural development. *Annu. Rev. Neurosci.* **21**, 309–345 (1998).
35. Paxinos, G. *The Rat Nervous System* (Academic, San Diego, California, 1995).
36. Walter, J., Henke-Fahle, S. & Bonhoeffer, F. Avoidance of posterior tectal membranes by temporal retinal axons. *Development* **101**, 909–913 (1987).
37. McCasland, J. S., Bernardo, K. L., Probst, K. L. & Woolsey, T. A. Cortical local circuit axons do not mature after early deafferentation. *Proc. Natl. Acad. Sci. USA* **89**, 1832–1836 (1992).
38. Chiaia, N. L. *et al.* Evidence for prenatal competition among the central arbors of trigeminal primary afferent neurons. *J. Neurosci.* **12**, 62–76 (1992).
39. Renehan, W. E., Crissman, R. S. & Jacquin, M. F. Primary afferent plasticity following partial denervation of the trigeminal brainstem nuclear complex in the postnatal rat. *J. Neurosci.* **14**, 721–739 (1994).
40. Killackey, H. P., Chiaia, N. L., Bennett-Clarke, C. A., Eck, M. & Rhoades, R. W. Peripheral influences on the size and organization of somatotopic representations in the fetal rat cortex. *J. Neurosci.* **14**, 1496–1506 (1994).
41. Fox, K. A critical period for experience-dependent synaptic plasticity in rat barrel cortex. *J. Neurosci.* **12**, 1826–1838 (1992).
42. Gao, W. Q. *et al.* Regulation of hippocampal synaptic plasticity by the tyrosine kinase receptor, Rek7/EphA5, and its ligand, AL-1/ephrin-A5. *Mol. Cell. Neurosci.* **11**, 247–259 (1998).
43. Rakic, P. Specification of cerebral cortical areas. *Science* **241**, 170–176 (1988).
44. O'Leary, D. D. M. Do cortical areas emerge from a protocortex? *Trends Neurosci.* **12**, 400–406 (1989).
45. Miyashita-Lin, E. M., Hevner, R., Wassarman, K. M., Martinez, S. & Rubenstein, J. L. R. Early neocortical regionalization in the absence of thalamic innervation. *Science* **285**, 906–909 (1999).
46. Crair, M. C., Gillespie, D. C. & Stryker, M. P. The role of visual experience in the development of columns in cat visual cortex. *Science* **279**, 566–570 (1998).
47. Crowley, J. C. & Katz, L. C. Development of ocular dominance columns in the absence of retinal input. *Nat. Neurosci.* **2**, 1125–1130 (1999).
48. Winslow, J. W. *et al.* Cloning of AL-1, a ligand for an Eph-related tyrosine kinase receptor involved in axon bundle formation. *Neuron* **14**, 973–981 (1995).
49. Wong-Riley, M. Changes in the visual system of monocularly sutured or enucleated cats demonstrable with cytochrome oxidase histochemistry. *Brain Res.* **171**, 11–28 (1979).
50. Schlaggar, B. L., De Carlos, J. A. & O'Leary, D. D. M. Acetylcholinesterase as an early marker of the differentiation of dorsal thalamus in embryonic rats. *Dev. Brain Res.* **75**, 19–30 (1993).